https://doi.org/10.1016/j.apenergy.2019.01.159

Submitted to *Applied Energy*
(Original Research Ms)

Revised Ms. APEN-D-18-04250

Development and characterization of novel and stable silicon nanoparticles-embedded PCM-in-water emulsions for thermal energy storage

Xiyao Zhang [a], Jianlei Niu [b], Jian-yong Wu [a] *

[a] Department of Applied Biology & Chemical Technology, The Hong Kong Polytechnic University, Hung Hom, Kowloon, Hong Kong

[b] Faculty of Architecture, Design and Planning, The University of Sydney, Sydney, Australia

* Corresponding author: jian-yong.wu@polyu.edu.hk

Abstract A phase change material (PCM) emulsion was formed by dispersing the PCM in water with the aid of emulsifiers, which had higher fluidity, higher thermal conductivity, and more flexible volume change than the solid-liquid PCMs. However, a critical issue for their large-scale applications is phase instability due to aggregation and precipitation of the PCM droplets. This work was to develop stable PCM emulsions prepared with n-hexadecane by manipulating the key factors and analysing the emulsion properties including emulsifier combinations and process conditions, interfacial film properties, droplet size distribution, and rheology characteristics. The stability was improved further with the addition of SiO_2 nano-particles. The SiO_2 nano-particles also acted as an effective nucleating agent to reduce the degree of supercooling. The thermal performance for potential application in thermal energy storage systems was also examined. Eventually, a novel and highly stable PCM-in-water nano-emulsions with droplets on a scale of tens of nanometers was developed for potential application in thermal energy storage systems.

Keywords: PCM emulsion; Nano-emulsion; Nano-particle; Stability; Viscosity; Supercooling.

1. Introduction

Thermal energy storage (TES) systems are widely used worldwide for efficient utilization and conservation of off-peak power, waste heat and intermittent energy sources [1]. In comparison of the two common heat storage methods, sensible and latent heat storage, the latent heat storage (LHS) provides a much greater energy storage density and a much smaller temperature difference between the storage and release of heat. LHS is accomplished by phase change materials (PCM) which absorb and release latent heat during phase change at a constant temperature. However, the application of PCM is restricted by several major technical issues such as the low thermal conductivity [2], the high degree of supercooling [3], the instability of performance during temperature cycles [4], and the erosion of containers [5-7].

PCM emulsions that are formed by dispersing PCM droplets in a liquid such as water can improve the heat transfer by increasing the surface-to-volume ratio of the PCM [8, 9]. The PCM emulsions remain in a fluid state throughout the phase change process, allowing for easy pump transportation and circulation in the energy storage systems. Compared with the

other two common fluid storage media including ice slurries and microencapsulated PCM (MPCM) slurries, the PCM emulsions are more efficient because the production of ice requires high energy expense while the microcapsule shell increases the cost and heat transfer resistance.

Maintaining the stability of dispersion is a major challenge in the development and application of PCM emulsions. The instability of emulsions can be attributed to several processes as follows [10, 11]. The most common process is creaming resulting from the accumulation of oil droplets and formation of an oil layer on the liquid surface (or sedimentation if the oil is heavier). Other causes of instability include phase inversion and Ostwald ripening, due to the solubility difference of the dispersed droplets of different sizes. Creaming, flocculation, and coalescence are the most frequent instability phenomena in PCM emulsions [12, 13]. A typical instability process is the partial coalescence occurring during phase changes in PCM emulsions [14]. The crystal growth of PCM can break the interfacial films between aggregated droplets, leading to the formation of a separated oil layer in the subsequent thawing process. Therefore, the instability problem is more prevalent in LHS applications than in other service fields of emulsions. Among these instability mechanisms, creaming and flocculation processes are reversible in which the size distribution of droplets does not change. Coalescence leads to the accumulation of droplets and its recovery requires extra energy [15].

Several strategies have been proposed to improve the stability of PCM emulsions. Use of appropriate emulsifiers at suitable concentrations is the first essential strategy for maintaining uniform and stable droplets. It has been suggested that use of mixed nonionic emulsifiers to form denser interfacial layers can stabilize paraffinic emulsions by the steric effect [14] and the emulsifier concentrations must be sufficient to cover the droplets entirely [16]. Stable emulsions of small and uniform droplets have been prepared with suitable formulations and process conditions according to the principles of colloid and surface chemistry [17, 18]. PCM emulsions with different droplet sizes have been prepared with an ultrasonic generator and a rotor-stator device and the emulsions with smaller droplets were more stable [19]. Particularly, the nano-emulsions of nano-sized droplets (20-500 nm) of PCM dispersed in water stabilized with emulsifiers have a superior stability [20-22]. Schalbart et al. (2010) produced a tetradecane nano-emulsion with small droplets in the range of 200-250 nm, which showed

good stability and low viscosity [23]. Polymer surfactants [24] and amphipathic solid particles [25, 26] have been reported to enhance the interfacial film strength as emulsifiers in emulsions. A higher viscosity of the continuous phase increases the stability by slowing down the aggregation of droplets [10], though it is not favorable for fluid transportation through the piping system and convective heat transfer. Manipulating the environmental conditions such as the storage temperature and the external forces also contribute to the stabilization of emulsion [27, 28].

Emulsion instability is attributed to multiple factors through complex relationships. Although different strategies have been reported, a more systematic assessment of the major physicochemical factors and better understanding of the physical mechanisms of their effects on the emulsion properties. This study aimed to develop a novel and stable PCM-water nano-emulsion through a systematic assessment of the major factors affecting the stability, and to elucidate the physical principles for improving the stability of PCM emulsions for thermal storage applications. The effects of different emulsifier systems, emulsifier concentrations, dispersed phase contents, and preparation process conditions on the emulsion properties were evaluated. The stability of emulsions was evaluated over extended periods of time and multiple freeze-thaw cycles. The physical principles and theoretical basis were carefully elaborated for understanding the factor effects on stability. The performance factors for their potential application in TES systems were examined, including the thermal performance, the degree of supercooling and rheology characteristics.

2. Materials and methods

2.1 Materials

The major PCM chemical, n-hexadecane, $C_{16}H_{34}$, (99%), was purchased from International Laboratory (USA). Commercial non-ionic surfactants including the hydrophilic Tween and the hydrophobic Span series including Tween 20, Tween 80, Span 20, Span 80, and an ethoxylate (EO) type surfactant, polyoxyethylene (4) lauryl ether, were chosen in this work for stabilizing the PCM emulsions (from Aladdin and Sigma-Aldrich in analytical grade). Hydrophobic nano SiO_2 particles were used as the nucleating agent (NA). The SiO_2 particles in a diameter range of 7 nm to 40 nm were purchased from Aladdin, China (Hydrophobic-230, 99.8% metal basis).

2.2 Preparation of PCM emulsions

The n-hexadecane was mixed with deionized water at a given mass ratio. The emulsifiers (mixtures of Tween and Span at mass ratios selected according to the HLB numbers) and the SiO_2 nano-particles were then added to the mixture. The mixtures were homogenized with an Ultra-Turrax T25 (IKA-Labor-Technik) for 10 min at room temperature for emulsion formation.

Emulsions were prepared in six sets of conditions as shown in Table 1. The mass ratio of emulsifiers was adjusted to attain the desired HLB values according to $HLB_{mix} = HLB_T \cdot M_T\% + HLB_S \cdot M_S\%$, where HLB_T and HLB_S are the HLB values of Tween 80 (15.0), Span 80 (4.3) at 25 °C, respectively, $M_T\%$ and $M_S\%$ the wt% of Tween 80 and Span 80, respectively.

2.3 Preparation of PCM nano-emulsions

The PCM nano-emulsions were prepared by the phase inversion temperature (PIT) method [29]. Water was added slowly (approximately 1.0 mL min^{-1}) into a mixture of n-hexadecane and selected emulsifiers with agitation on a magnetic stirrer at 400-600 rpm and the temperature maintained above 50 °C. N-hexadecane concentration was fixed at 30 wt% in all emulsions, whereas the surfactant concentration was varied in each sample. The liquid mixture was cooled down to room temperature, yielding the PCM-in-water nano-emulsions. Two types of nano-emulsions were prepared by this method, one being emulsified by the mixture of Tween 80 and Span 80 and the other by a non-ionic surfactant of the ethoxylate type.

2.4 Analysis of emulsion droplets

The size distribution of emulsion droplets was analyzed by dynamic laser scatter (DLS) using Malven Zetasizer model 3000HSA instrument, having a broad measuring range from 0.02 μm to 5,000 μm. A total of 100 measurements were taken for 20 min at a scattering angle of 90° at 25 °C. The average particle size (in nm) and the polydispersity index were determined using the Zetasizer 3000HSA-Advanced Software. The morphology of the PCM emulsion

was examined using a Leica DM4000 optical microscope at a magnification range of 400×-1,000×. The images were processed using the Leica LAS AF software.

2.5 Thermal analysis

The melting and nucleation temperatures of PCM emulsion samples were measured with a differential scanning calorimeter (METTLER TOLEDO DSC-822e) with aluminum crucibles. The thermal data was analyzed and plotted using the STARe software. Temperature and sensitivity calibrations were conducted using standard materials at a heating/cooling rate of 5 °C/min. The samples were maintained at an initial temperature of −5 °C for 10 min to facilitate stabilization, heated to 30 °C, maintained at 30 °C for 10 min, and finally cooled to −5 °C.

The onset temperature for melting and crystallization is defined as the temperature at which the first crystallites melt or form, can be observed as a deviation from the baseline, and is independent of the heating/cooling rates [30]. Therefore, the difference between onset temperatures for melting and crystallization was regarded as the supercooling degree of the samples.

2.6 Viscosity

The viscosity of emulsions was determined using a rotational viscometer with an ultra-low viscosity adapter (Brookfield, DV-E), which can measure the viscosity of Newtonian fluids and the apparent viscosity of non-Newtonian fluids. The measurement range of this device is from 6.4 mPa·s to 2,000,000 mPa·s, and its accuracy is +/−1%. Since the emulsions displayed non-Newtonian fluid behavior, the apparent viscosity at a low shear rate (0.6 s^{-1} at 0.5 rpm) was determined.

2.7 Evaluation of the stability of the PCM emulsion

The storage stability of emulsions was evaluated based on the droplet size distribution and phase separation of the samples observed during the storage period and repeated thermal cycles. According to the standard procedure for testing the stability of PCM emulsions under cooling and heating thermal cycles [31], the emulsion sample was first cooled in an ice-water

bath at 0 °C for 30 min, and then warmed to room temperature (~25 °C) for 30 min. The emulsion sample was poured into a stoppered 10 mL cylindrical bottle immediately after preparation. After ten freeze-thaw cycles, the breaking ratio (volume ratio of the separated oil phase to the total volume of the emulsion) was determined by the following equation to compare the degree of stability of the different emulsion samples.

$$\text{Breaking ratio} = h_o/(X_{pcm}\cdot \text{H}) \times 100 \qquad (1)$$

where X_{pcm} is the original volume fraction of the PCM in the emulsion, H the total height of the emulsion in the glass tubes prior to the test, and h_o the height of the oil layer measured after the freeze-thaw cycles. Three measurements were taken for each emulsion sample and the average value was recorded.

3 Results and discussion

3.1 Effects of emulsifier systems on emulsion properties and stability

The effects of various non-ionic emulsifiers on the droplet diameter distribution, apparent viscosity, and stability of the emulsions were evaluated to select a suitable emulsifier system. The PCM-water mixture was successfully emulsified with all combinations of Tween and Span surfactants by homogenization at 8,000 rpm. <Figure 1a shows the average droplet size of the PCM emulsions with different emulsifiers, being the smallest with Tween 20-Span 20 of 889.8 nm and the largest with Tween 20-Span 80 of 1,367.8 nm. All emulsions had a wide droplet size distribution (PDI = 1).

<Figure 1>

The samples were subjected to multiple freeze-thaw cycles to evaluate their stability. After the thermal treatment, a separated oil layer appeared over the emulsion in all samples; this phenomenon indicates the emulsion breaking. The separated oil layers arose in all samples after around two cycles and continued to grow after repeated thermal cycles. The increase in the volume of the separated oil phase slowed down after four cycles. The stability of the

PCM emulsion was evaluated by comparing the volume ratio of the oil layer to the total PCM after ten freeze-thaw cycles.

<Figure 1a also shows the volume ratios of the separated oil layer to the total PCM in the emulsion samples for different emulsifiers after 10 freeze-thaw cycles. With the lowest ratio of 8.0 ± 2.7%, the Tween 80-Span 80 emulsion was the most stable. The Tween 80-Span 20 emulsion with a ratio of 17.1 ± 5.6% was also quite stable. The other two samples with ratios higher than 70% were unstable. Thus, Tween 80 and Span 80 were finally selected as the emulsifiers for the subsequent investigation because of the good stability of their emulsion sample.

<Figure 1b shows the variation in apparent viscosity at different shear rates of the emulsion samples homogenized at 8,000 rpm. All emulsion samples exhibited the similar shear-thinning characteristic of a pseudoplastic fluid and their apparent viscosity decreased with the shear rate.

3.2 Relationship of emulsifier stability to HLB value

Emulsion samples with 30 wt% PCM and 5.0 wt% emulsifiers of a mixture of Tween 80 and Span 80 at different mixing ratios were prepared at 25 °C. As shown in <Figure 2, emulsions with droplet diameters below 1,500 nm were achieved with the HLB value controlled below 11. The relatively low breaking ratios of PCM samples in the HLB range from 9.5 to 11 indicates a better stability than with the samples with beyond this HLB range. As the HLB value increased, the average droplet diameter increased and the stability decreased of the samples. The droplet size is a determining factor on the stability of the emulsion. The optimum HLB range from 9.5 to 11 is in agreement with the results reported in the literature [17]. The mass ratio of Tween 80 to Span 80 at 1:1 having an HLB number of 9.65 within the optimum range was applied in the following experiments.

<Figure 2>

3.3 Effects of emulsifier concentration

The emulsifier concentration affects the surface tension and the droplet size, and also the emulsion stability and the viscosity. As shown in **Error! Reference source not found.**a, the average droplet size gradually declined as the emulsifier concentration increased while the breaking ratio of emulsion declined (or stability increased).

<Figure 3>

At a low emulsifier concentration of 1 wt%, the emulsifier molecules were insufficient to cover the entire oil-water interface and to decrease the interface tension. As a result, the average droplet size was large, and the emulsion distribution was wide. Therefore, the amount of emulsifier must exceed a critical value to coat the emulsion droplets entirely. Emulsion stability can be promoted by an interface film with densely arranged emulsifier molecules and small droplet sizes. Thus, high stability was observed in the samples with high concentrations of emulsifiers.

As shown in **Error! Reference source not found.**b, the apparent viscosity-shear rate trend of all emulsion samples exhibited a pseudoplastic fluid behavior. With the increase in emulsifier concentration, the apparent viscosity at different shear rates increased, due probably to a significant increase in the emulsifier content in the continuous phase. The stability of the emulsion samples reached a steady level at 5 wt%, which was chosen as the optimum concentration of the emulsifiers.

3.4 Effects of the PCM content

A relatively high PCM content is desirable for achieving a high density of heat storage. Emulsion samples with different PCM contents were compared to determine the optimum in the emulsion. As shown in Figure 4a, the average droplet diameters of samples increased from about 500 nm to 2,200 nm with the PCM content. Moreover, the breaking ratio of the emulsion samples indicated an intensified trend, reaching to more than 20% for a PCM content of 50 wt% (Figure 4a). The apparent viscosity of the emulsion increased accordingly (Figure 4b). Thus, the instability caused by droplet collisions in the samples with high PCM content could not be restrained by a similar level of viscosity in low-content samples.

Consequently, samples with high PCM content displayed poor stability. Thus, the PCM concentration of 30 wt% was recommended in this case to balance the stability and heat storage density.

<Figure 3>

3.5 Effects of emulsification methods

PCM emulsions with different droplet sizes were obtained by varying the homogenization shear rates from 8,000 rpm to 24,000 rpm (<Figure 4a). Two types of PCM nano-emulsions were also prepared and compared with those prepared by the high-energy emulsification method. All samples had a unimodal, approximately lognormal distribution function. The average droplet diameter of the PCM emulsion homogenized at 8,000 rpm was 1,259 ± 52.9 nm, with a broad distribution (PDI = 1). Approximately 8.0 ± 2.7% of the PCM droplet volume in this sample was broken during the repeated freeze-thaw cycles. When the homogenization rate was increased to 9,500 rpm, the average droplet size of the emulsion significantly decreased to 774.3 ± 24.5 nm with a narrow distribution, and further decreased to 467.2 ± 16.6 nm at 24,000 rpm. As for the PCM nano-emulsion, the sample with Tween 80 and Span 80 had an average diameter of 319.3 ± 2.9 nm, whereas the sample with the EO emulsifier had a much smaller droplet size of 78.2 ± 8.2 nm in a narrow range. Moreover, all samples except for the that prepared at 8,000 rpm showed a good stability during the freeze-thaw cycles with no distinct separated oil layer after 10 cycles.

<Figure 4b shows the apparent viscosity-shear rate trends of the emulsion samples. The emulsifier concentration mainly affected the apparent viscosity, rather than the droplet size. The samples prepared at 8,000 rpm and 24,000 rpm exhibited the similar trend. However, the nano-emulsion sample with Tween 80 and Span 80 displayed a slightly high apparent viscosity because of its higher emulsifier content (10 wt%). The large number of droplets also results in a high viscosity. Despite the high emulsifier concentration, the nano-emulsions at a low shear rate range behaved as a Newtonian fluid with a low apparent viscosity, especially for the emulsions formed with the EO surfactant. The simple flow behavior is more favorable for engineering applications with a great potential in active heat transfer AC systems,

improving chiller energy efficiency by quick charging and extending the life circle of energy storage media.

<Figure 4>

3.5 Stability of the PCM emulsion during the storage period

The PCM emulsion samples obtained by five different emulsification methods were stored at room temperature over three months during which observation was made daily (<Figure 5). Creaming appeared in the sample homogenized at 8,000 rpm in several days, and in samples homogenized at 13,500 and 24,000 rpm in about four weeks, but never in the samples prepared by the PIT method. Sample e remained translucent through the storage period, indicating that the size of droplets maintained shorter than the visible wavelength (390 nm). According to the Stokes equation ($v_{stokes} = \frac{2\Delta\rho g\, r^2}{9\eta}$), creaming can be reduced by reducing the droplet size or increasing the viscosity with a thickener [32]. Therefore, the small and uniform droplet size distribution contributed to the excellent storage stability of emulsions prepared by the PIT method.

<Figure 5>

3.7 Morphology of emulsion samples

<Figure 6a shows the microscopic photographs of a PCM emulsions prepared with Tween 80-Span 80 which was homogenized at 8,000 rpm. The size and shape of the droplets were consistent with the results obtained by DLS, with an outer diameter ranging from 0.1 to 10 μm. As shown in <Figure 6b, the sample prepared by the same method with 1 wt% of nano SiO_2 particles contained aggregated droplet clusters, as deduced in Section 3.6. The nano-emulsion prepared by the PIT method with Tween 80-Span 80 (<Figure 6c) contained much smaller droplets.

<Figure 6>

3.8 Effects of nanoparticles on stability and supercooling of PCM emulsion

Supercooling occurs when a liquid starts to freeze at a temperature below its melting temperature and is usually more serious in small volumes such as in emulsion droplets [19, 33]. The addition of solid impurities as the seeds for nucleation and crystal growth by the heterogeneous nucleation is a common approach to minimizing supercooling, such as solid compounds with similar structures [18, 34, 35] and carbon/oxide particles [3, 36, 37]. In the present study, hydrophobic SiO_2 nanoparticle was used as the nucleating agent as it suppressed supercooling effectively in our previous work [38]. Moreover, small solid particles can also aid surfactant molecules to form interfacial films on the droplet interface which can stabilize the emulsion [39]. However, a solid stabilized emulsion tends to have a high viscosity, which is unfavorable for engineering applications.

As shown in <Figure 7, when a small amount (0.5 wt%) of nano SiO_2 was added to the emulsion, the stability and apparent viscosity of the emulsion was not affected markedly. However, the stability (low breaking ratio) and apparent viscosity were increased sharply with 1 wt% or more of the nanoparticles. With 2 wt% of nano SiO_2, the apparent viscosity of the emulsion samples was over 10,000 mPa·s, suggesting the severe aggregation of the emulsion droplets. But the aggregation did not result in the emulsion breaking by the partial coalescence during freeze-thaw cycles. The results suggest that the increase in stability of emulsion with the nanoparticles was probably attributed to the increase in viscosity. The high viscosity is not desirable for LHS applications. Therefore, the use of solid particles in high concentrations in the PCM emulsions is not a favorable strategy in terms of the fluidity.

<Figure 7>

<Figure 8>

The effect of SiO_2 nanoparticles on supercooling was evaluated in the emulsion prepared at 8,000 rpm with Tween 80 and Span 80. <Figure 8 shows the reduction of supercooling with the nanoparticles during the phase change process and Table 1 shows the corresponding melting and crystallization properties. Without the nucleating agent, a high degree of supercooling of 14.5 °C was observed. When the concentration of nucleating agent was low, two distinct peaks were noted in the freezing curves, suggesting that the amount of nucleating agent was insufficient to disperse all of the droplets. As the mass concentration of the nucleating agent increased, the second peak above 15 °C gradually increased, whereas the first peak decreased. In the samples with nucleating agent concentration of more than 1 wt%, most of the PCM droplets were crystallized above 15 °C, and the onset temperatures were approximately the same as in the bulk PCM. Thus, the degree of supercooling was well controlled to approximate 1°C at a nucleating agent concentration from 1 wt% to 2 wt%, which is a relatively lowe value compared with the effeteness of NAs in literatures [18, 40, 41]. As the addition of nanoparticles also increased the viscosity of the emulsion, the optimal concentration of the nano SiO_2 nucleating agent was approximately 1 wt% for good fluidity.

4 General discussion

Emulsion is a thermodynamically unstable system due to the large interfacial area [42]. Emulsion instability is represented by the decrease in the number of emulsion droplets as a result of flocculation or coalescence, whose rate is defined as the product of collision frequency and collision efficiency [42]. Individual droplets collide because of their movements that can be induced by Brownian motion, gravitational field (buoyancy), and other mechanical forces [11, 15]. For spherical droplets at relatively small fluctuation density, the collision frequency is predicted by the von Smoluchowski theory [43]. The collision frequency driven by Brownian motion is given by [44],

F —— (2)

The frequency driven by gravitational force is given by [45],

—— —— (3)

where η represents the viscosity of the continuous phase, k Boltzmann constant, T absolute temperature, $\Delta\rho$ the difference in the densities of the dispersed and continuous phases, and γ the shear rate. The theory assumes that all collided droplets are spherical in shape with the same radius r_i in a unit volume of emulsion with a dispersion phase volume fraction of Φ_i [46, 47].

4.1 Droplet size distribution

The size of emulsion droplets can usually be reduced by increasing the emulsifier concentration (lowering the interfacial tension) by using specific emulsifiers or controlling the preparing methods, such as applications of the high-speed homogenization and the phase inversion method. Although the equation (3) predicts that small droplets collide more frequently than larger ones due to Brownian movements, the present study showed stable emulsions were attained with small droplets at a moderate viscosity, because that the gravitational effect on micro-sized droplets far-exceeds the Brownian diffusion: $\frac{4}{3}\pi R^3 \Delta\rho g L \gg kT$ (where k is the Boltzmann constant and T the absolute temperature; L is the height of the container.) When the droplet size is in the range of few 100 nm and the density difference Δρ is minimal, the gravitational movement is restrained [10]. In addition, the Stokes equation ($V_{stokes} = \frac{2\Delta\rho g\, r^2}{9\eta}$) indicates that the rate of gravitational separation increases with the particle size [48]. Therefore, creaming develops quickly in the emulsion with large droplets such that the dispersed droplets are concentrated in the creaming layer. According to Equation (2), the development rate of instability in concentrated emulsions accelerates, which might be the major reason of stable emulsions with small droplets. Furthermore, Equation (3) indicates that gravitational collision increases as the difference between the droplet sizes increases. The collision frequency for gravitationally induced aggregation was reduced in emulsions with uniform droplets, which also contributed to this result. The nano-emulsions usually exhibits good stability against creaming, sedimentation, flocculation, and coalescence because of less gravitational affection and non-deformable interfaces with minimal curvature radii [49].

The curvature of the liquid film region determines the Laplace pressure (the interfacial normal stress balance): $\Delta P_L = 2\sigma/r$, where σ is the interfacial tension and r is the curvature

radius [32]. Thus, larger forces are needed to deform or break up smaller droplets. The Weber number ($We = \frac{2\eta\gamma}{\Delta P_L} = \frac{\eta\gamma r}{\sigma}$) is a dimensionless number that is often useful in analyzing multiphase flows with strongly curved surfaces [50]. A sufficient shear force is needed to exceed a critical value We_{cr} (of the order of one) to break up a droplet and it increases with the droplet size decreasing, which also is the reason of the good stability of small droplets.

4.2 Viscosity

Based on the results of previous sections, the viscosity of an emulsion sample increase with the emulsifier concentration increasing, PCM mass fraction increasing and the droplet size decreasing. Comparison of the results in Sections 3.6 reveals that the emulsion with a high solid particle content exhibited a better coalescence stability and a much greater apparent viscosity than the emulsion with low concentrations of nanoparticles. The high apparent viscosity contributes to this effect by limiting the movement of the droplets, and the thickening is more effective than control of droplet size in stabilizing emulsions in this case. However, a high apparent viscosity is undesirable in a TES system. Moreover, We_{cr} depends on the type of flow and on the ratio of the droplet viscosity to that of the continuous phase (η_d/η_c), and it decreases with the viscosity ratio approaching 1. In this case, the viscosity of n-hexadecane is reported to be 3.45 at 20°C which was much lower than that of the continual phase [51]. Thus, the critical value We_{cr} increases with the emulsion viscosity.

4.3 Stabilizers and interfacial films

The interfacial properties of an emulsion involve the interfacial tension, the interfacial viscosity, the interfacial elasticity, the thickness of the interfacial film, and the mechanical strength. It has been proved that the emulsion stability is independent of the interfacial tension, but it mainly depends on the rest natures [52].

Emulsifiers keep emulsions stable by reducing the interfacial tension between the two layers and inducing the interface films for preventing coalescence [16, 53]. The formation and stabilization of emulsion depend strongly on emulsifiers. As demonstrated in Section 3.1, after emulsion formation, the non-ionic emulsifier molecules adsorbed onto droplet surfaces prevent instability by steric repulsion, which is dependent on the emulsifier molecular

structure. The increase in emulsifier concentration leads to the decrease in surface tension and average droplet size as well as the increase in molecular absorption, interfacial viscosity, and the thickness, thereby enhancing emulsion stability. Once the concentration exceeds the critical micelle concentration (CMC), the emulsifier molecules stop absorbing onto the surface and aggregate into micelles such that emulsion viscosity drastically increases. At concentrations much greater than CMC, surfactants micelles form multi-layer structures parallel to interfacial surfaces, which further enhances the stability of emulsion [54, 55]. Furthermore, solid particles and/or polymer surfactant could generate dense interfacial films with high interfacial strength resulting in highly stable emulsions (Section 3.6). The physicochemical stability of emulsifiers is also important which may affect the thermal stability and service life of the interfacial film. Therefore, the effect of emulsifier type on the stability of the emulsion is a result of combined factors, and no apparent relationship exists between emulsion stability and the average droplet diameters of the emulsion samples with different emulsifiers.

The combination of some emulsifiers may lead to much lower surface tension than used individually. The presence of more than one surfactant molecule at the interface tends to increase the strength of interfacial films from a consideration of the steric repulsion that produces more stable films in multi-layer structures [56]. HLB numbers of emulsifier systems reflect the balance of the emulsifier molecular at the oil-water interface. Lipophilic emulsifiers at low HLB numbers tend to form an adsorption layer in the oil phase, and vice versa. The multi-layer structure of emulsifiers contributes a protective effect against the film drainage during the coalescence process, especially the lipophilic layer in the oil phase which is hard to be detached from the film drainage.

When the emulsion droplets collide with each other, the path leads to a slight flattening deformation of the interface of two droplets and a thin liquid film (the dimple shaped region) forms between the drops. Further approach elevates the pressure in the liquid film which starts to drain trapped the liquid of external phase. The film drainage imposes strong shear forces on the emulsifier interface resulting in a concentration gradient of the emulsifier molecules [57]. If the process is sufficiently slow, the gradient of the interfacial tension resulted from the emulsifier concentration generates a tangential stress at the droplet interfaces against the film drainage, namely, the Marangoni effect [58]. The multi-layer

structure or high viscosities of emulsifiers slows down the film drainage rate, which enables emulsifier molecules to have enough time to rearrange in the interfacial film. Otherwise, when the film becomes very thin or forms ‘hollow spaces’, intermolecular forces or interface fluctuations (Mechanical vibrations and thermal fluctuations) might break up the thin film, thus, coalescence occurs [59-61].

4.4 Water-oil ratio

A highly dispersed phase content accelerated instability, as shown in Section 3.4. However, the viscosity of the emulsions increased with the disperse phase content, and the emulsion samples with a high PCM mass fraction was observed to be stable in our previous work [38]. According to the von Smoluchowski theory, a high volume fraction of the dispersed phase enhances the collision probability and frequency between droplets. On the other hand, a high viscosity can also improve emulsion stability by restricting the movement of the droplets. All these mechanisms can contribute to the droplet collision frequency in an emulsion. In practice, one of these mechanisms is usually more dominant than the rest, depending on the composition of the product and its effect on viscosity. In our cases, at a low dispersed phase content (< 25 wt%), the effect of viscosity dominates. However, at a highly dispersed phase content, the effects caused by the concentrated droplets of the emulsion are dominant.

4.5 Environmental factors

Temperature has shown a negative effect on emulsion stability in our previous work on PCM emulsion with a higher melting temperature [38]. Increase in temperature speeds up the Brownian motion of droplets and lowers the fluid viscosity, leading to emulsion instability. Meantime, the interface viscosity also drops and the energy fluctuation at the liquid films of flocculated droplets is intensified at a higher temperature. In addition, temperature changes may result in phase transition processes, breaking the emulsion by partial coalescence. Temperature can also affect the emulsion properties. For example, non-ionic surfactants of the ethoxylate type are highly dependent on temperature, becoming lipophilic with increasing temperature due to the dehydration of the polyethylene oxide chain, which are commonly

used in preparing nano-emulsions (Section 3.5). Therefore, temperature changes can induce phase inversion in emulsions.

Another example is that the CMC values of surfactants are related to the temperature; specifically, the CMC values decrease to a minimum first and then increases with the increase in temperature. The increase in temperature results in a decline in the hydration of the hydrophilic group, thereby improving micellization. However, it also causes the breakage of the structured water surrounding the hydrophobic group, which suppresses micellization [28]. The relative magnitude of the two opposing effects determines the CMC value at a particular temperature. According to previous reports [62, 63], the minimum CMC values is approximately 25 °C for ionic and 50 °C for non-ionic surfactants.

Gravity is the most significant factor for instability in normal poly-dispersed emulsions. The collisions due to gravity induced concentrates and different vertical velocities of the droplets lead to most of their instability issues directly or indirectly. However, in nano-emulsions, Brownian motion becomes more significant than the gravity effect [49]. The mechanical shear force reduces the apparent viscosity of emulsions with non-Newtonian behaviors, promoting collision. On the other hand, external shear force can also break up droplets into smaller ones if the force was sufficient to overcome interface free energy and the Laplace pressure, depending the critical Weber number We_{cr}.

5 Conclusions

In this work, n-hexadecane in water emulsions were prepared with various emulsifier combinations for evaluation of the influencing factors on emulsion stability. Suitable emulsifiers and concentration protect emulsion droplets from aggregation and further coalescence. A small-sized and uniform distribution decreased the creaming speed and the gravitationally induced aggregation such that the PCM emulsion stabilized. A moderate apparent viscosity limits the movement of the droplets and avoids their collisions, which sometimes is more effective than controlling the droplet size to stabilize emulsions. However, a high viscosity is undesirable in TES systems.

An optimum emulsion formula has been derived, Tween 80 and Span 80 at mass ratio 1/1 as the emulsifiers at 5 wt%, and 30 wt% PCM for good stability and the fluidity. The latent heat of the emulsions was 62.23 kJ/kg, and the freezing temperature was 17 °C. Supercooling was efficiently suppressed by using hydrophobic SiO_2 nanoparticles as the nucleating agent. The shear thinning property of a pseudoplastic fluid was observed in all samples, and most of them displayed good fluidity. It is concluded from the experimental results that the following three approaches are effective for improving the stability of the PCM emulsion, (1) using mixed emulsifiers; (2) reducing the droplet size and distribution, and (3) maintaining a suitable viscosity. A novel n-hexadecane-based PCM nano-emulsion has been developed with a minimum average droplet size at 78.2 ± 8.2 nm with superior stability. It is has the potential for application in active heat transfer AC systems to raise chiller energy efficiency and extend the life circle of energy storage media.

Acknowledgments

This work was supported financially by the Research Grant Council of the Hong Kong SAR Government through RGC General Research Fund (PolyU 152707/16E) and by the Hong Kong Polytechnic University.

References

[1] Farid MM, Khudhair AM, Razack SAK, Al-Hallaj S. A review on phase change energy storage: materials and applications. Energy Conversion and Management. 2004;45:1597-615.

[2] Sarı A, Karaipekli A. Thermal conductivity and latent heat thermal energy storage characteristics of paraffin/expanded graphite composite as phase change material. Applied Thermal Engineering. 2007;27:1271-7.

[3] Zhang X, Niu J, Zhang S, Wu J-Y. PCM in Water Emulsions: Supercooling Reduction Effects of Nano-Additives, Viscosity Effects of Surfactants and Stability. Advanced Engineering Materials. 2015;17:181-8.

[4] Dinçer İ, Rosen MA. Thermal Energy Storage (TES) Methods. Thermal Energy Storage: John Wiley & Sons, Ltd; 2010. p. 83-190.

[5] Inaba H, Morita S-I. Cold heat-release characteristics of phase-change emulsion by air-emulsion direct-contact heat exchange method. International Journal of Heat and Mass Transfer. 1996;39:1797-803.

[6] Cabeza LF, Illa J, Roca J, Badia F, Mehling H, Hiebler S, et al. Immersion corrosion tests on metal-salt hydrate pairs used for latent heat storage in the 32 to 36°C temperature range. Materials and Corrosion. 2001;52:140-6.

[7] Zalba B, Marín JM, Cabeza LF, Mehling H. Review on thermal energy storage with phase change: materials, heat transfer analysis and applications. Applied Thermal Engineering. 2003;23:251-83.

[8] Delgado M, Lázaro A, Mazo J, Zalba B. Review on phase change material emulsions and microencapsulated phase change material slurries: Materials, heat transfer studies and applications. Renewable and Sustainable Energy Reviews. 2012;16:253-73.

[9] Lu W, Tassou SA. Experimental study of the thermal characteristics of phase change slurries for active cooling. Applied Energy. 2012;91:366-74.

[10] Tadros T. Application of rheology for assessment and prediction of the long-term physical stability of emulsions. Adv Colloid Interface Sci. 2004;108-109:227-58.

[11] Isaacs EE, Chow RS. Practical Aspects of Emulsion Stability. In: Schramm LL, editor. Washington, D.C.: American Chemical Society; 1992. p. 51-77.

[12] Huang L, Petermann M, Doetsch C. Evaluation of paraffin/water emulsion as a phase change slurry for cooling applications. Energy. 2009;34:1145-55.

[13] van Boekel MAJS, Walstra P. Stability of oil-in-water emulsions with crystals in the disperse phase. Colloids and Surfaces. 1981;3:109-18.

[14] Golemanov K, Tcholakova S, Denkov ND, Gurkov T. Selection of surfactants for stable paraffin-in-water dispersions, undergoing solid-liquid transition of the dispersed particles. Langmuir. 2006;22:3560-9.

[15] Tadros TF. Emulsion Formation and Stability: John Wiley & Sons; 2013.

[16] Choi E, Cho YI, Lorsch HG. Effects of emulsifier on particle size of a phase change material in a mixture with water. International Communications in Heat and Mass Transfer. 1991;18:759-66.

[17] Boyd J, Parkinson C, Sherman P. Factors affecting emulsion stability, and the HLB concept. Journal of Colloid And Interface Science. 1972;41:359-70.

[18] Huang L, Günther E, Doetsch C, Mehling H. Subcooling in PCM emulsions—Part 1: Experimental. Thermochimica Acta. 2010;509:93-9.

[19] Günther E, Schmid T, Mehling H, Hiebler S, Huang L. Subcooling in hexadecane emulsions. International Journal of Refrigeration. 2010;33:1605-11.

[20] Izquierdo P, Esquena J, Tadros TF, Dederen C, Garcia M, Azemar N, et al. Formation and stability of nano-emulsions prepared using the phase inversion temperature method. Langmuir : the ACS journal of surfaces and colloids. 2002;18:26-30.

[21] Liu W, Sun D, Li C, Liu Q, Xu J. Formation and stability of paraffin oil-in-water nano-emulsions prepared by the emulsion inversion point method. J Colloid Interface Sci. 2006;303:557-63.

[22] Chen J, Zhang P. Preparation and characterization of nano-sized phase change emulsions as thermal energy storage and transport media. Applied Energy. 2017;190:868-79.

[23] Schalbart P, Kawaji M, Fumoto K. Formation of tetradecane nanoemulsion by low-energy emulsification methods. International Journal of Refrigeration. 2010;33:1612-24.

[24] Park H, Han DW, Kim JW. Highly stable phase change material emulsions fabricated by interfacial assembly of amphiphilic block copolymers during phase inversion. Langmuir. 2015;31:2649-54.

[25] Chevalier Y, Bolzinger MA. Emulsions stabilized with solid nanoparticles: Pickering emulsions. Colloids and Surfaces A: Physicochemical and Engineering Aspects. 2013;439:23-34.

[26] Dickinson E. Food emulsions and foams: Stabilization by particles. Current Opinion in Colloid & Interface Science. 2010;15:40-9.

[27] Degner BM, Chung C, Schlegel V, Hutkins R, McClements DJ. Factors Influencing the Freeze-Thaw Stability of Emulsion-Based Foods. Comprehensive Reviews in Food Science and Food Safety. 2014;13:98-113.

[28] Rosen MJ, Kunjappu JT. Surfactants and Interfacial Phenomena. 4th ed. Hoboken, NJ, USA: John Wiley & Sons, Inc.; 2012.

[29] Anton N, Gayet P, Benoit JP, Saulnier P. Nano-emulsions and nanocapsules by the PIT method: An investigation on the role of the temperature cycling on the emulsion phase inversion. International journal of pharmaceutics. 2007;344:44-52.

[30] Höhne GWH, Hemminger WF, Flammersheim HJ. Differential Scanning Calorimetry. Berlin, Heidelberg: Springer Berlin Heidelberg; 2003.

[31] Coupland JN. Crystallization in emulsions. Current Opinion in Colloid and Interface Science. 2002;7:445-50.

[32] Binks BP. Modern aspects of emulsion science: Royal Society of Chemistry; 1998.

[33] Mehling H, Cabeza LF. Heat and cold storage with PCM: Springer; 2008.

[34] Kishimoto A, Setoguchi T, Yoshikawa M, Nakahira T. Study on Thermal Properties of O/W Emulsions Type Latent Heat Tranportation Media. Proceedings of 16th Japan Symposium on Thermophysical Properties1995. p. 233-40.

[35] Zhang XX, Fan YF, Tao XM, Yick KL. Crystallization and prevention of supercooling of microencapsulated n-alkanes. Journal of Colloid and Interface Science. 2005;281:299-306.

[36] Wang F, Zhang C, Liu J, Fang X, Zhang Z. Highly stable graphite nanoparticle-dispersed phase change emulsions with little supercooling and high thermal conductivity for cold energy storage. Applied Energy. 2017;188:97-106.

[37] He J-P, Li H-M, Wang X-Y, Gao Y. In situ preparation of poly (ethylene terephthalate)–SiO2 nanocomposites. European Polymer Journal. 2006;42:1128-34.

[38] Zhang X, Wu J-y, Niu J. PCM-in-water emulsion for solar thermal applications: The effects of emulsifiers and emulsification conditions on thermal performance, stability and rheology characteristics. Solar Energy Materials and Solar Cells. 2016;147:211-24.

[39] Aveyard R, Binks BP, Clint JH. Emulsions Stabilized Solely by Colloidal Particles. Advances in colloid and interface science. 2003;100-102:503-46.

[40] Huang L, Doetsch C, Pollerberg C. Low temperature paraffin phase change emulsions. International Journal of Refrigeration. 2010;33:1583-9.

[41] Yang R, Xu H, Zhang Y. Preparation, physical property and thermal physical property of phase change microcapsule slurry and phase change emulsion. Solar Energy Materials and Solar Cells. 2003;80:405-16.

[42] McClements DJ. Food Emulsions: Principles, Practices, and Techniques, Third Edition: CRC Press; 2015.

[43] Smoluchowski MV. Drei Vorträge über Diffusion, Brownsche Molekularbewegung und Koagulation von Kolloidteilchen. Physik Zeit. 1916;17:557-85.

[44] Hiemenz PC, Rajagopalan R. Principles of Colloid and Surface Chemistry, Third Edition, Revised and Expanded: CRC Press; 1997.

[45] Zhang X, Davis RH. The rate of collisions due to Brownian or gravitational motion of small drops. Journal of Fluid Mechanics. 2006;230:479-504.

[46] Everett DH. Basic Principles of Colloid Science: Royal Society of Chemistry; 1988.

[47] Mollet H, Grubenmann A. Formulation technology: emulsions, suspensions, solid forms: John Wiley & Sons; 2008.

[48] Lamb H. Hydrodynamics. 6th ed. Cambridge: Cambridge University Press; 1993.

[49] Tadros T, Izquierdo P, Esquena J, Solans C. Formation and stability of nano-emulsions. Advances in colloid and interface science. 2004;108-109:303-18.

[50] Walstra P. Principles of emulsion formation. Chemical Engineering Science. 1993;48:333-49.

[51] Hardy RC. Viscosity of n-Hexadecane. Journal of Research of the National Bureau of Standards. 1958;61:433.

[52] Wasan D, Shah S, Aderangi N, Chan M, McNamara J. Observations on the coalescence behavior of oil droplets and emulsion stability in enhanced oil recovery. Society of Petroleum Engineers Journal. 1978;18:409-17.

[53] Vladisavljevic G. Influence of process parameters on droplet size distribution in SPG membrane emulsification and stability of prepared emulsion droplets. Journal of Membrane Science. 2003;225:15-23.

[54] Nikolov AD, Wasan DT. Ordered micelle structuring in thin films formed from anionic surfactant solutions. Journal of colloid and interface science. 1989;133:1-12.

[55] Nikolov AD, Wasan DT, Friberg SE. Effect of surfactant concentration on dispersion stability as probed by the film thickness stability mechanism. Colloids and Surfaces A: Physicochemical and Engineering Aspects. 1996;118:221-43.

[56] Ren Z. Study on relationship between interfacial surfactant structure and emulsion anti-coalescence stability (in Chinese). Zhejiang: Zhejiang University; 2000.

[57] Chesters AK. The modelling of coalescence processes in fluid-liquid dispersions : a review of current understanding. Chemical engineering research & design. 1991;69:259-70.

[58] Scriven L, Sternling C. The Marangoni Effects. Nature. 1960;187:186-8.

[59] Danov KD, Denkov ND, Petsev DN, Ivanov IB, Borwankar R. Coalescence dynamics of deformable Brownian emulsion droplets. Langmuir : the ACS journal of surfaces and colloids. 1993;9:1731-40.

[60] Ivanov IB. Effect of Surface Mobility on the Dynamic Behaviour of Thin Liquid Films. Pure and Applied Chemistry. 1980;52:1241-62.

[61] Ivanov I. Thin liquid films,Surfactant Science Series volume 29. New York and Basel: Marcel Dekker Inc; 1988.

[62] Crook E, Fordyce D, Trebbi G. Molecular weight distribution of nonionic surfactants. I. Surface and interfacial tension of normal distribution and homogeneous p, t-octylphenoxyethoxyethanols (OPE'S). The Journal of Physical Chemistry. 1963;67:1987-94.

[63] Flockhart B. The vapor pressures of ethanol-water solutions of detergents. Journal of Colloid Science. 1961;16:443-54.

Table 1 Experimental variables and conditions for preparation of PCM emulsions.

Tests of emulsifier mixtures	Total emulsifier	HLB value	PCM content	Emulsification methods
1. Tween (20, 80): Span (20, 80) at 1:1 mass ratio	5 wt%	By emulsifiers	30 wt%	Ultra-Turrax at 8, 000 rpm
2. Tween 80 and Span 80	5 wt%	8-14	30 wt%	Ultra-Turrax at 8, 000 rpm
3. Tween 80 and Span 80 at 1:1 mass ratio	1-9 wt%	9.65	30 wt%	Ultra-Turrax at 8, 000 rpm
4. Tween 80 and Span 80 at 1:1 mass ratio	1/6 of PCM mass	9.65	10-50 wt%	Ultra-Turrax at 8, 000 rpm
5. Tween 80 and Span 80 at 1:1 mass ratio	5 wt%	9.65	30 wt%	Ultra-Turrax at 8, 000 rpm-24,000 rpm
6. Tween 80 and Span 80 at 1:1 mass ratio + NA at 0-2 wt%	5 wt%	9.65	30 wt%	Ultra-Turrax at 24, 000 rpm

Table 2 Melting and freezing points of samples with nano SiO_2 as the nucleating agent.

Content (wt%)	ΔH_m (kJ/kg)	ΔH_f (kJ/kg)	$T_{m.onset}$ (°C)	$T_{f.onset}$ (°C)	ΔT (°C)
0	-50.2	51.2	18.1	3.6	14.5
0.5	-74.7	64.8	17.9	1^{st}: 17.1 2^{nd}: 3.8	0.8
1	-62.7	62.1	18.1	1^{st}: 17.0 2^{nd}: 2.9	1.1
1.5	-60.7	60.0	18.3	17.1	1.2
2	-62.9	62.1	18.3	17.0	1.3

ΔH_m and ΔH_f: the total transition enthalpies during the melting and crystallization processes, respectively; $T_{m.\ onset}$ and $T_{f.onset}$: the onset temperatures of the melting and crystallization processes, respectively; ΔT: degree of supercooling.

Figure Captions

Figure 1 Effects of emulsifiers on emulsion properties (under Test 1 conditions in Table 1): (a) Average droplet diameters of emulsion and breaking ratios of the PCM emulsions after 10 freeze-thaw cycles; (b) Apparent viscosity-shear rate curves at 25 °C. Error bars: standard deviation (SD) of triplicate experiments.

Figure 2 Average droplet size and breaking ratios of the PCM emulsions after 10 freeze-thaw cycles for emulsion samples with different HLB values of emulsifier systems (under Test 2 conditions in Table 1). Error bars: SD of triplicate experiments.

Figure 3 Effects of emulsifier concentration (under Test 3 conditions in Table 1): (a) Droplet size distribution; (b) Breaking ratio of the PCM emulsions; (c) Apparent viscosity-shear rate curves of emulsion samples with five different emulsifier concentrations at 25 °C. Error bars: SD of triplicate experiments.

Figure 4 Effects of the PCM content (under Test 4 conditions in Table 1): (a) Average droplet size and breaking ratio of the PCM emulsions; (b) Apparent viscosity-shear rate curves at 25 °C. Error bars: SD of triplicate experiments.

Figure 5 Effects of emulsification methods on (a) Droplet size distribution and (b) Apparent viscosity-shear rate curves at 25 °C of the emulsion and nano-emulsion samples prepared using different emulsification methods (under Test 5 conditions in Table 1, except for the nano-emulsions). Error bars: SD of triplicate experiments.

Figure 6 Photographs of the emulsion samples by different emulsification methods during the storage period: (a) homogenization at 8,000 rpm; (b) homogenization at 13,500 rpm; (c) homogenization at 24,000 rpm; (d) nano-emulsion with Tween 80 and Span 80; and (e) nano-emulsion with an EO surfactant.

Figure 7 Micromorphology of the emulsion droplets observed under an optical microscope (1000×): (a) prepared with Tween 80-Span 80 at 5 wt%, a PCM mass fraction of 20 wt%, and a homogenization rate of 8,000 rpm; (b) prepared by the same method plus the the addition of 1 wt% nano SiO_2; (c) nano-emulsion prepared by the PIT method with Tween 80-Span 80.

Figure 8 Effects of nanoparticles (under Test 6 conditions in Table 1): breaking ratio and apparent viscosities at a shear rate of 0.6 s^{-1} at 25 °C for the emulsion samples with different contents of nanoparticles, Error bars: SD of triplicate experiments.

Figure 9 DSC curves of the PCM emulsions with various concentrations of nano SiO_2 particles under Test 6 conditions in Table 1: (a) melting curves; (b) freezing curves.

Figure
Click here to download high resolution image

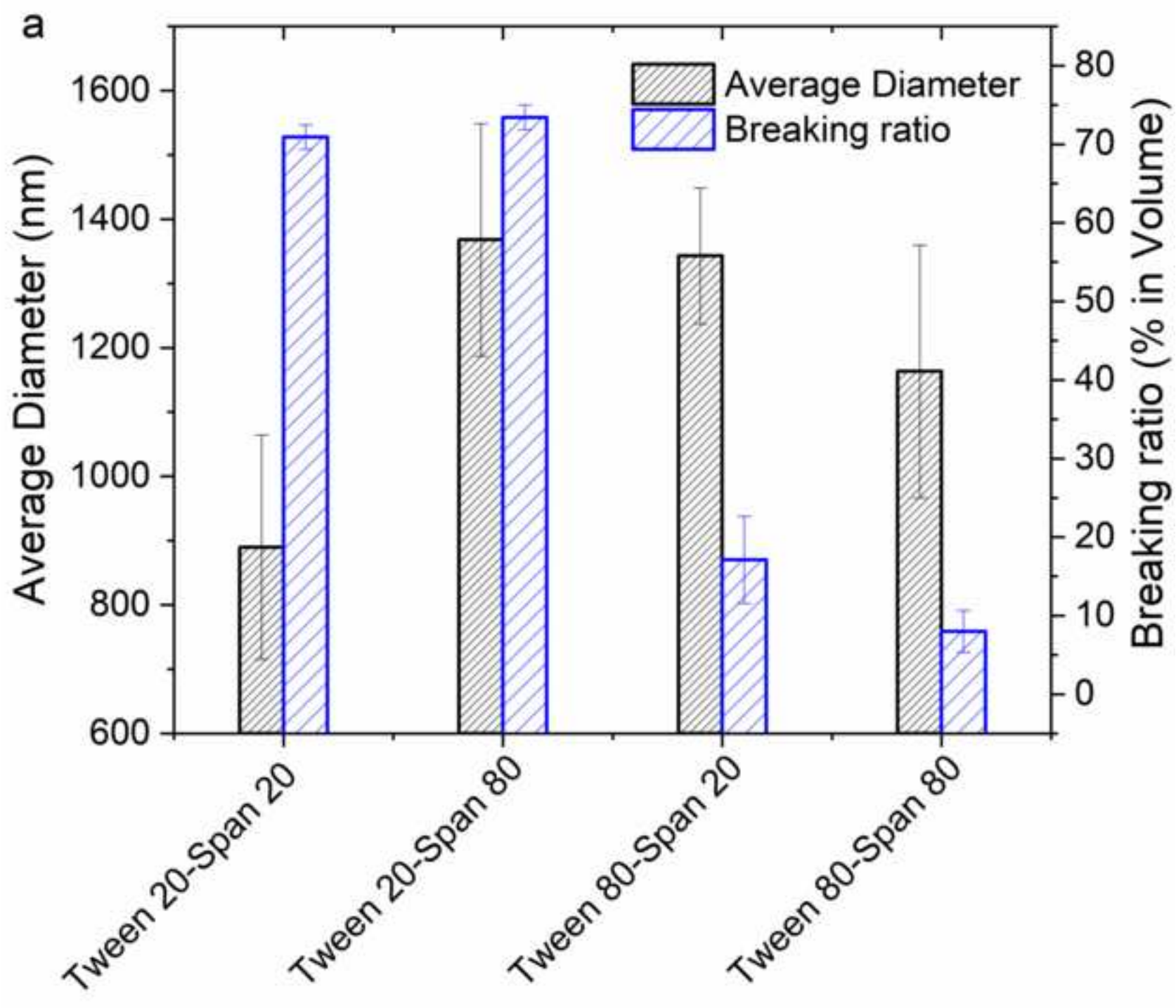

Figure
Click here to download high resolution image

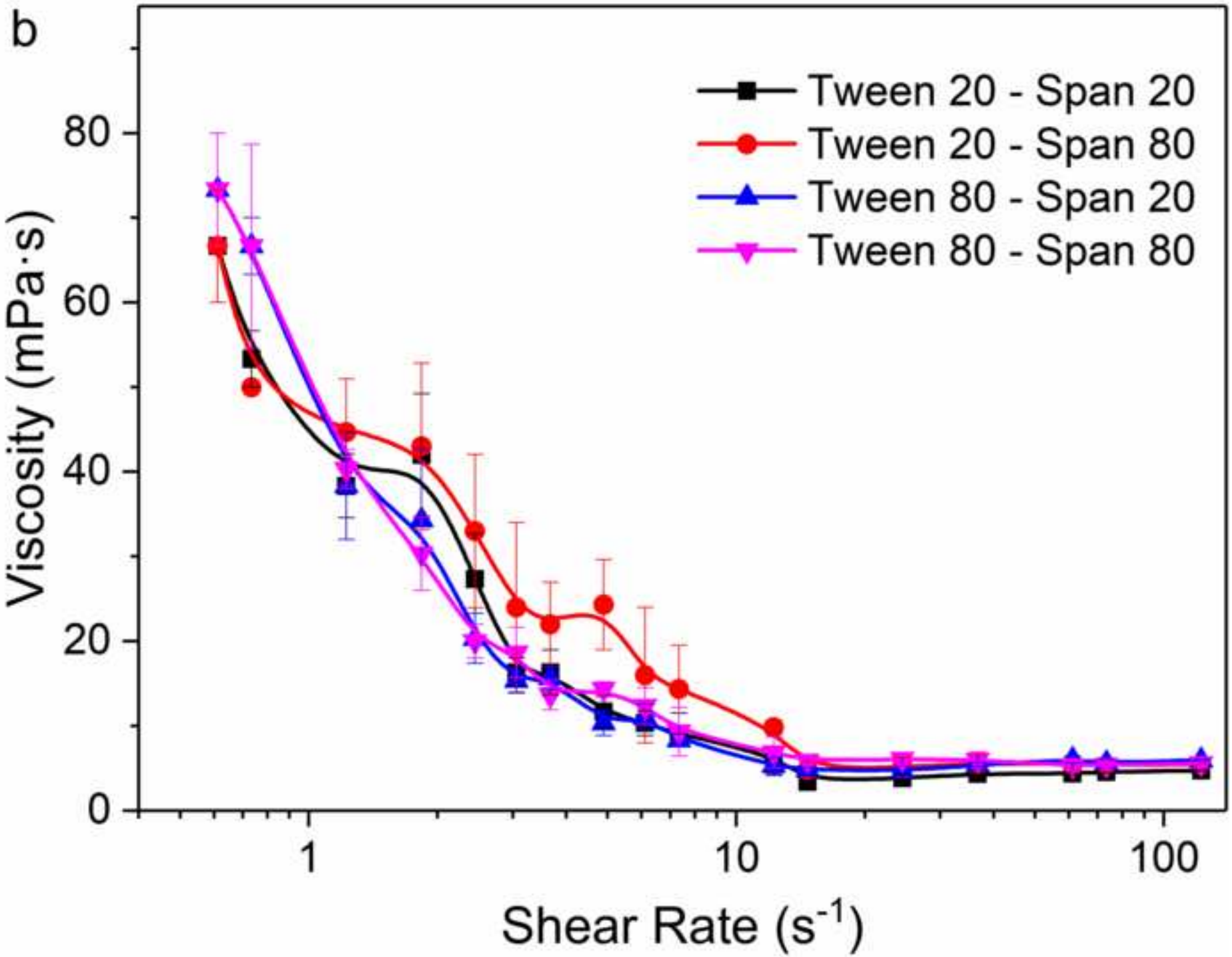

Figure

Click here to download high resolution image

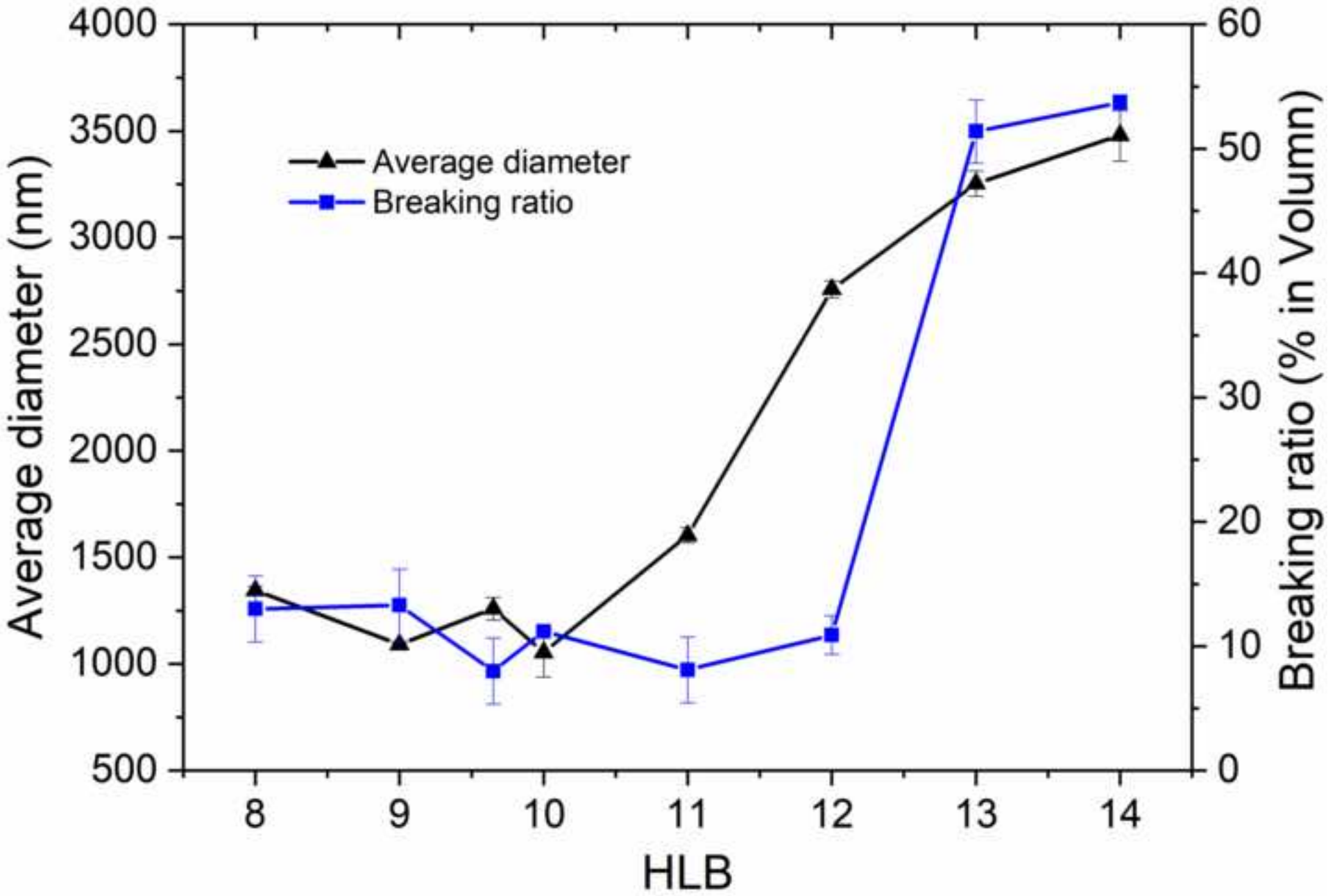

Figure

Click here to download high resolution image

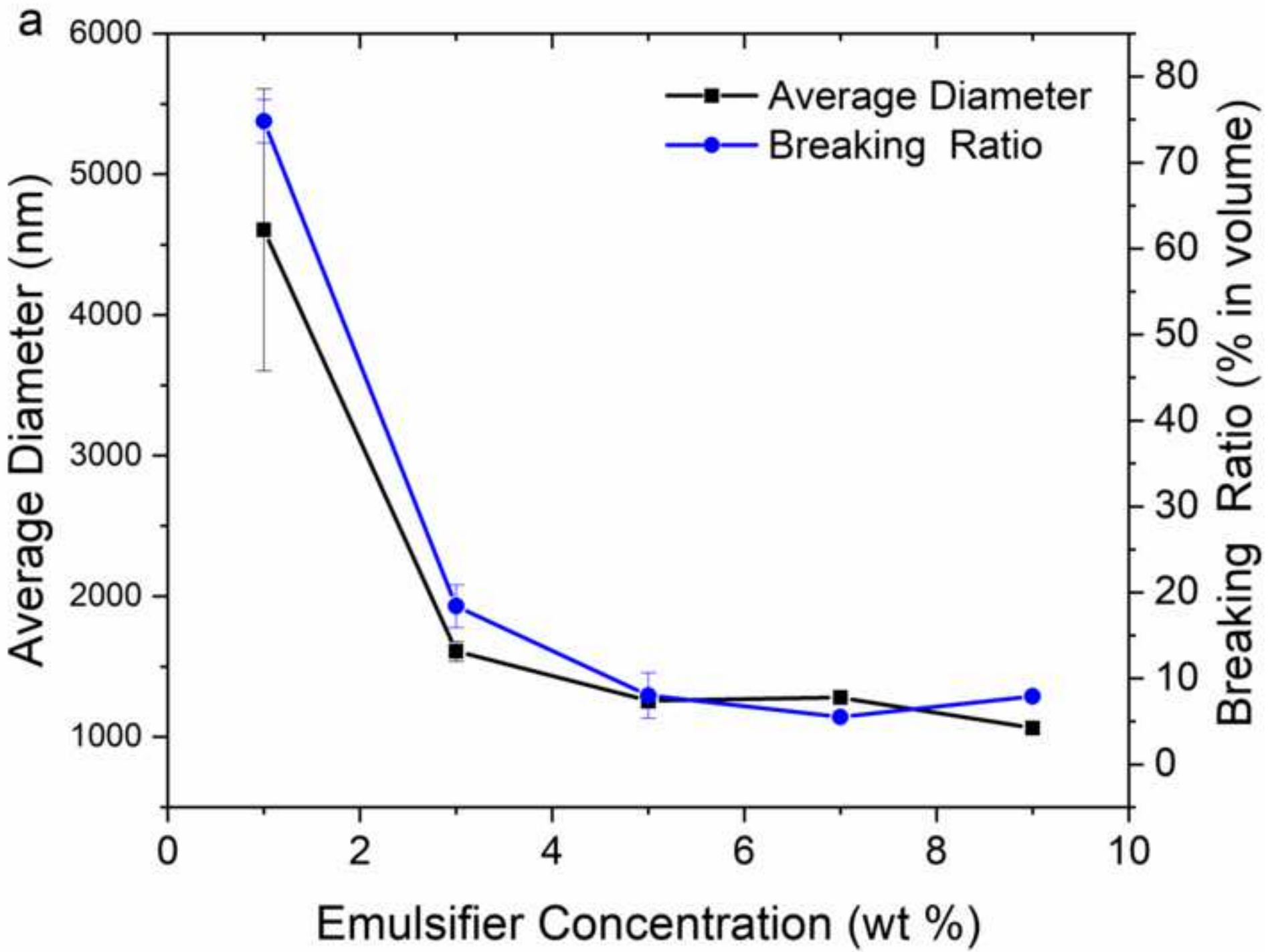

Figure
Click here to download high resolution image

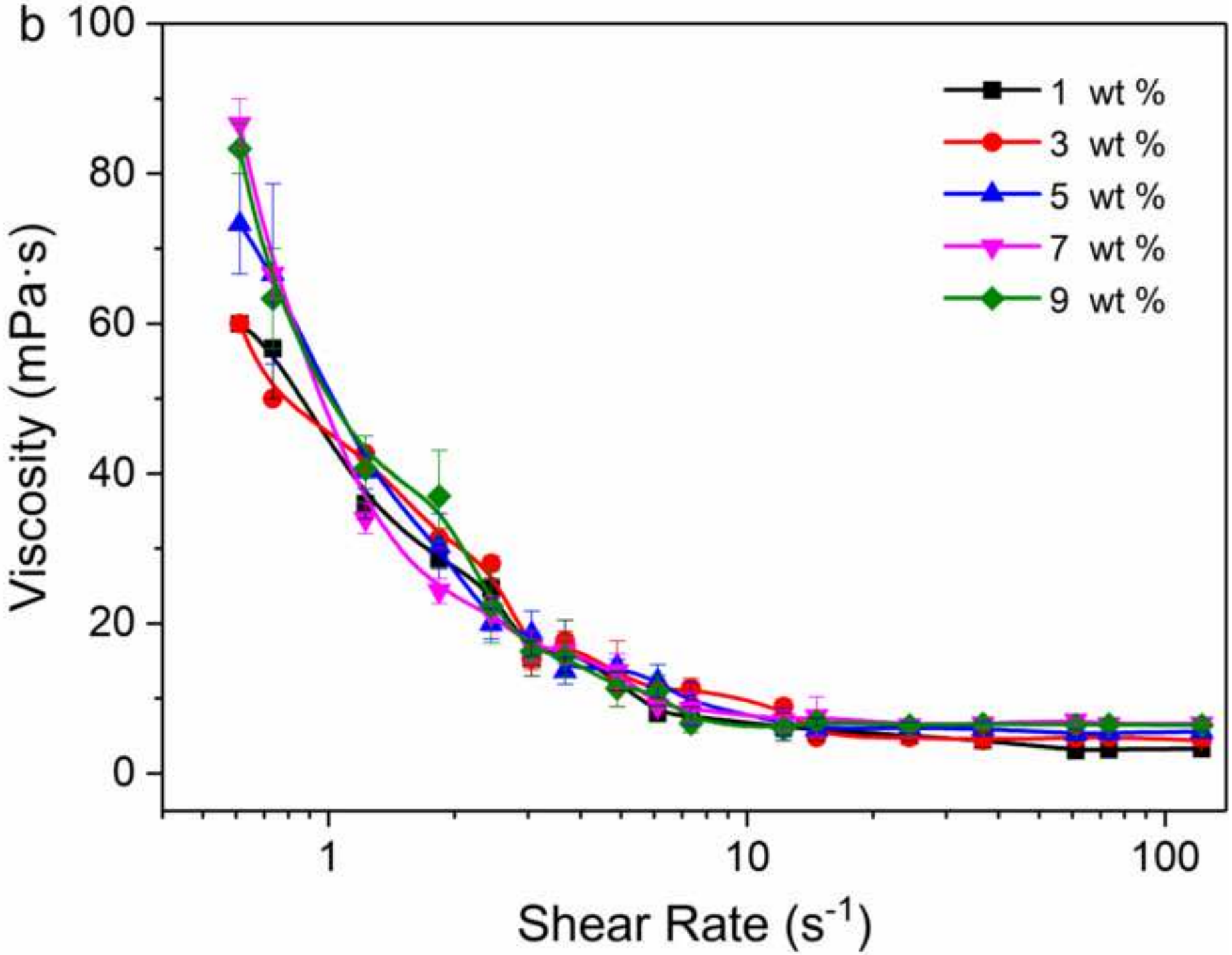

Figure

Click here to download high resolution image

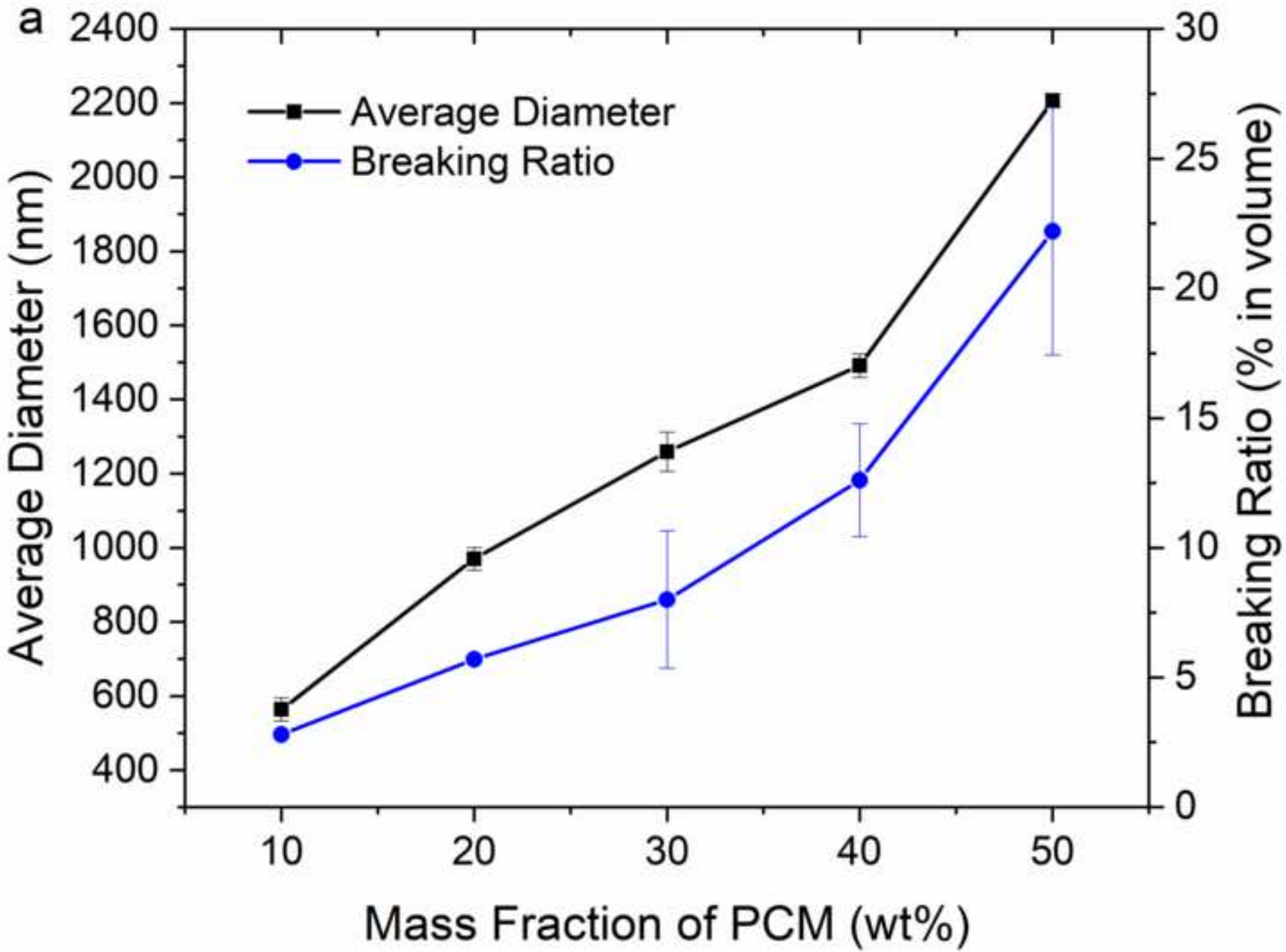

Figure
Click here to download high resolution image

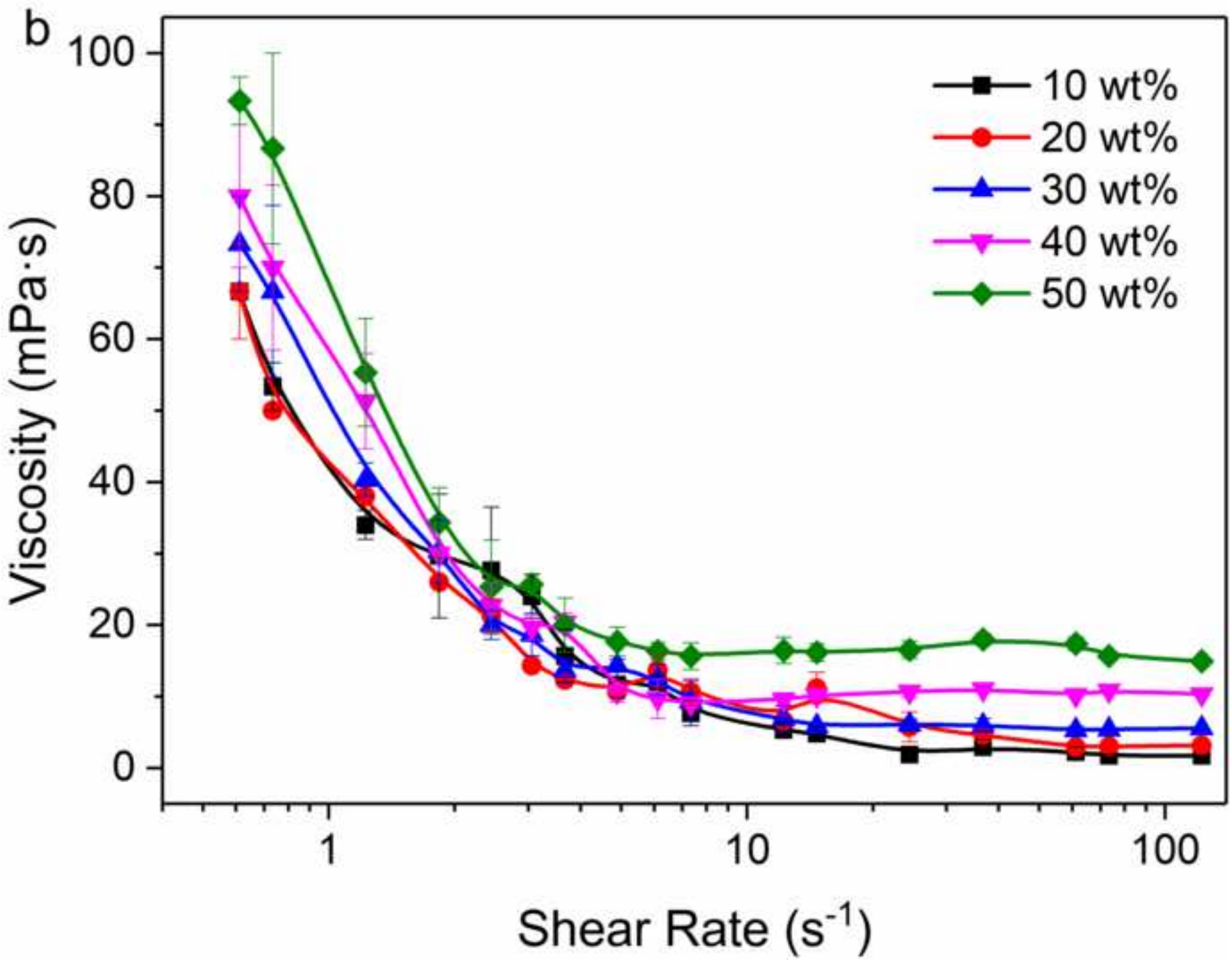

Figure

Click here to download high resolution image

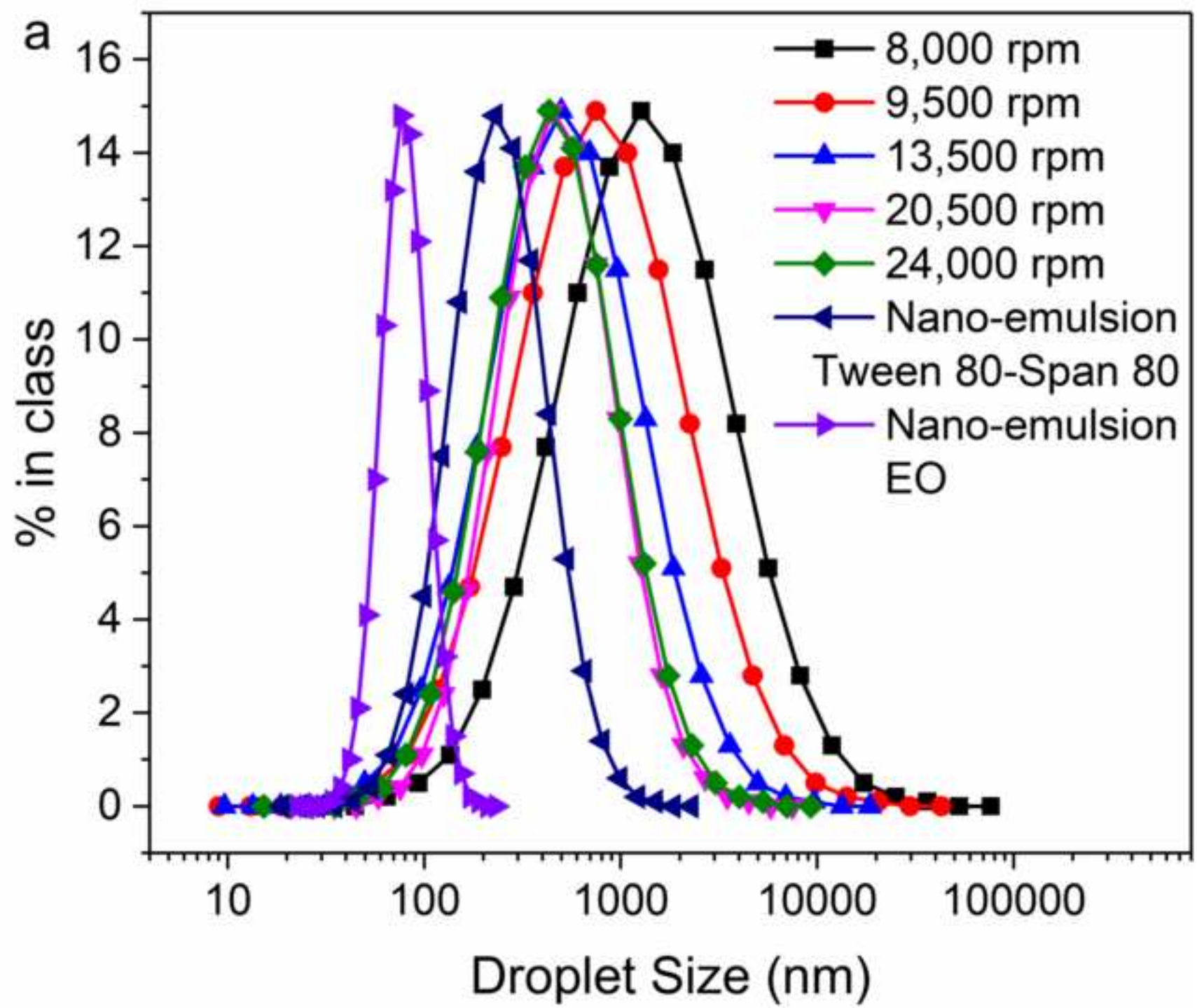

Figure

Click here to download high resolution image

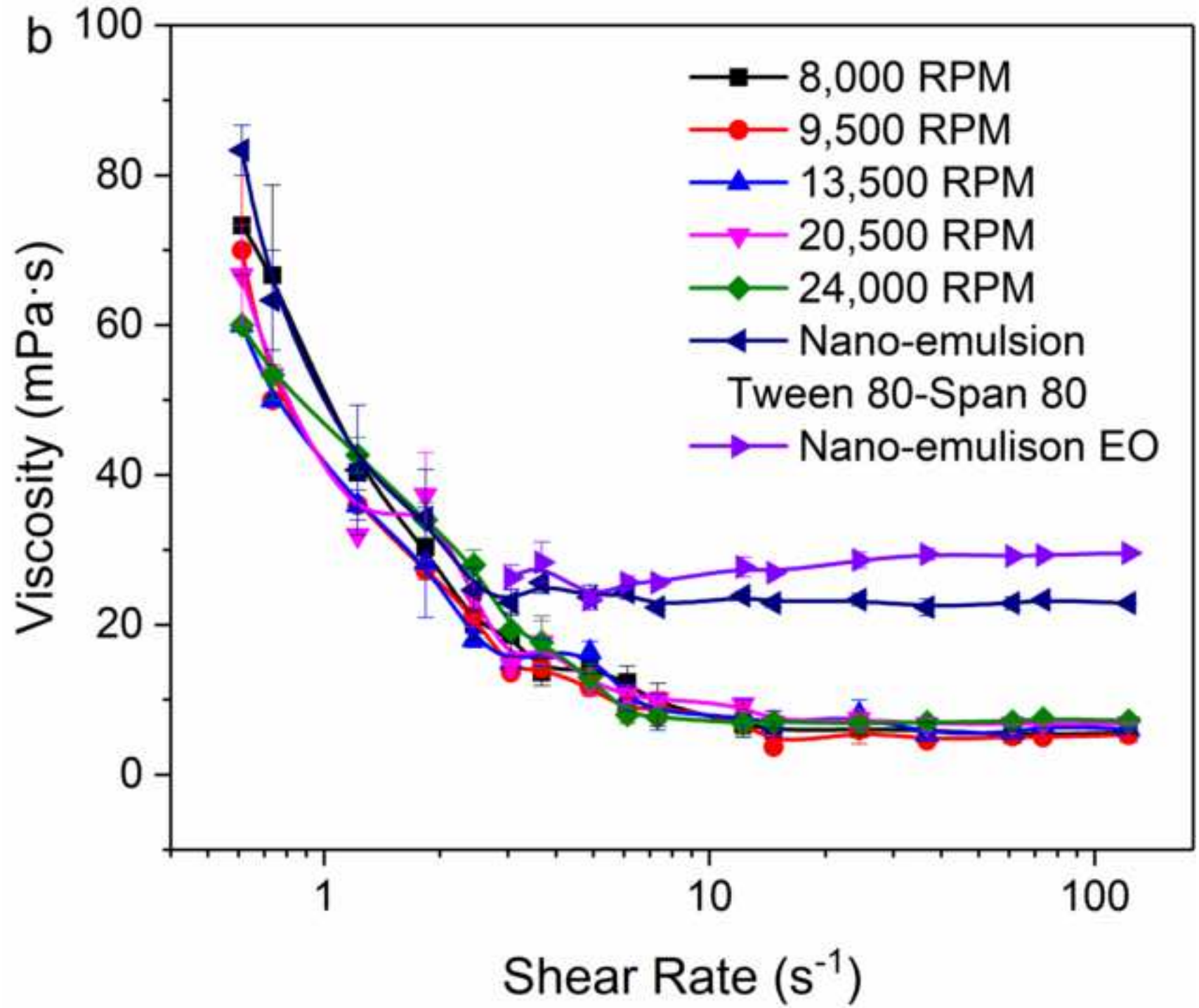

Figure
Click here to download high resolution image

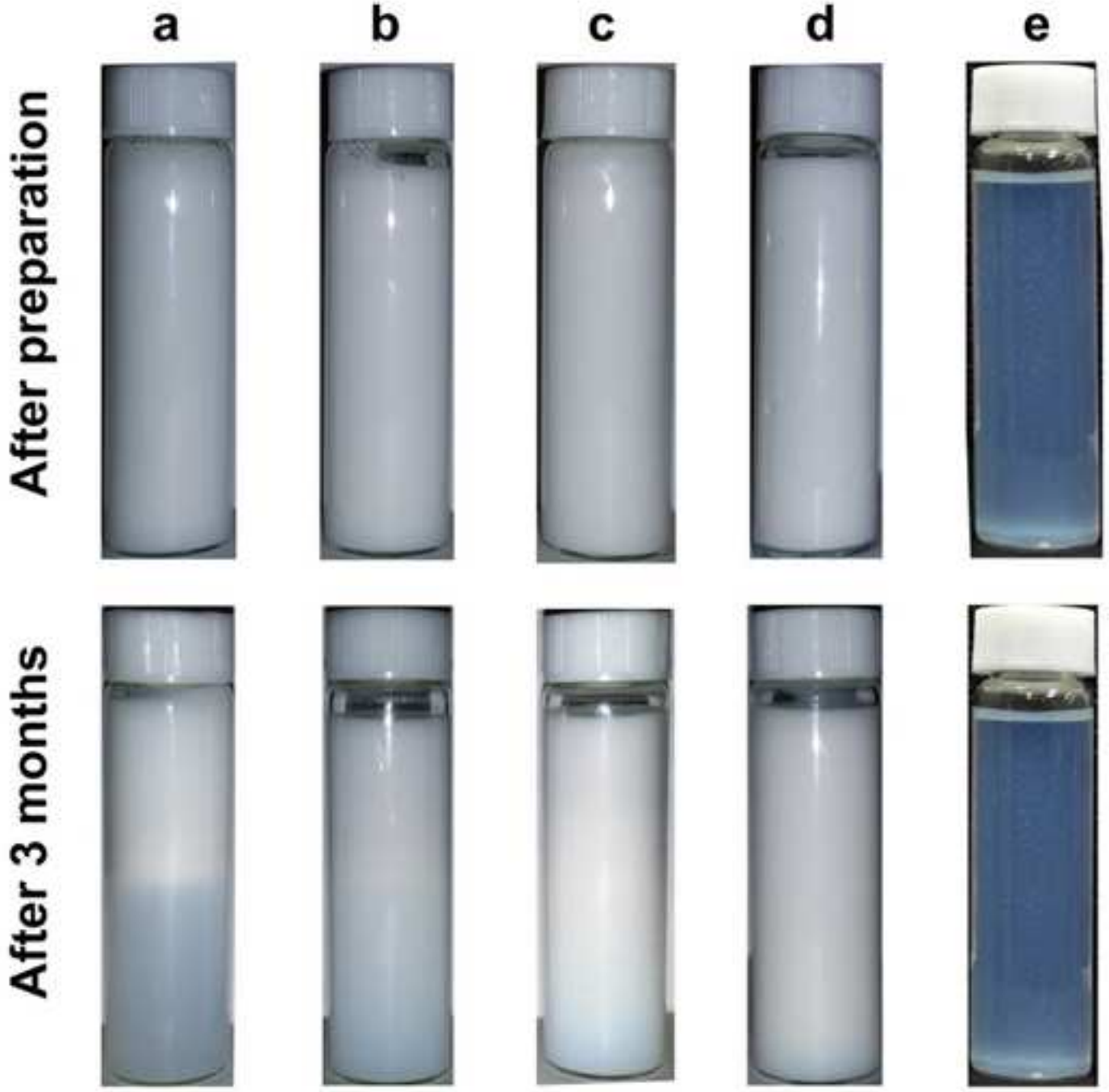

Figure

Click here to download high resolution image

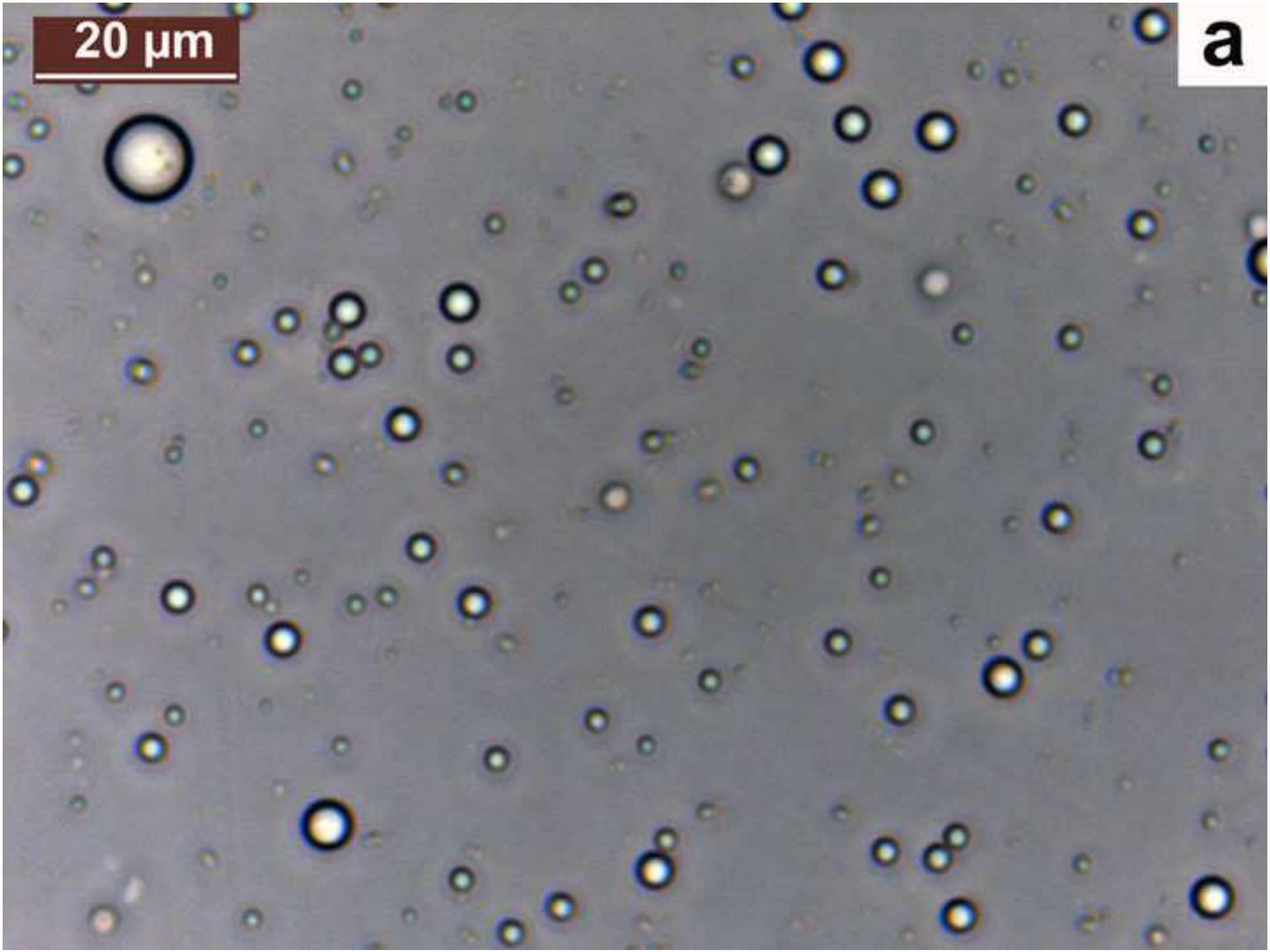

Figure

Click here to download high resolution image

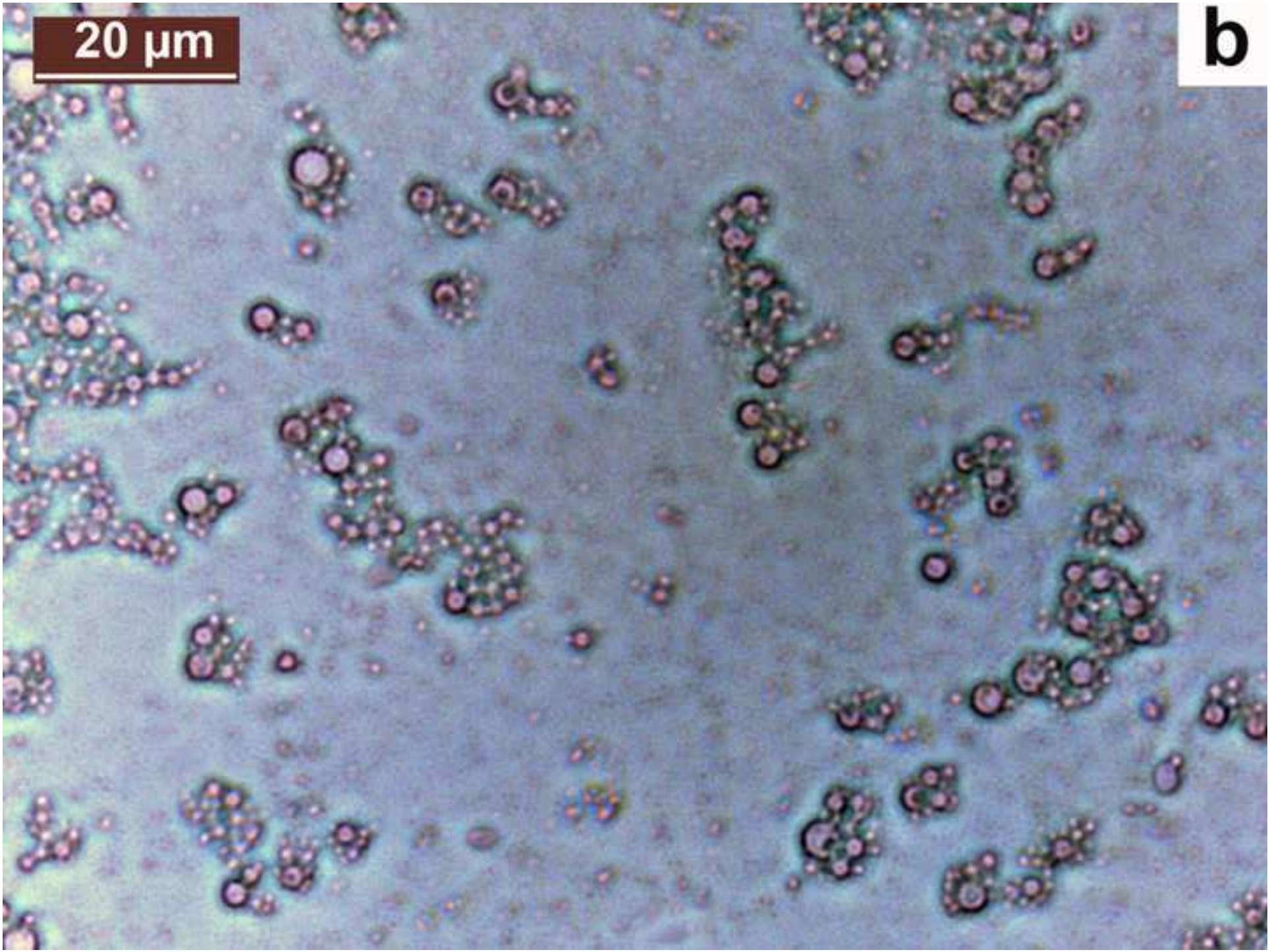

Figure

Click here to download high resolution image

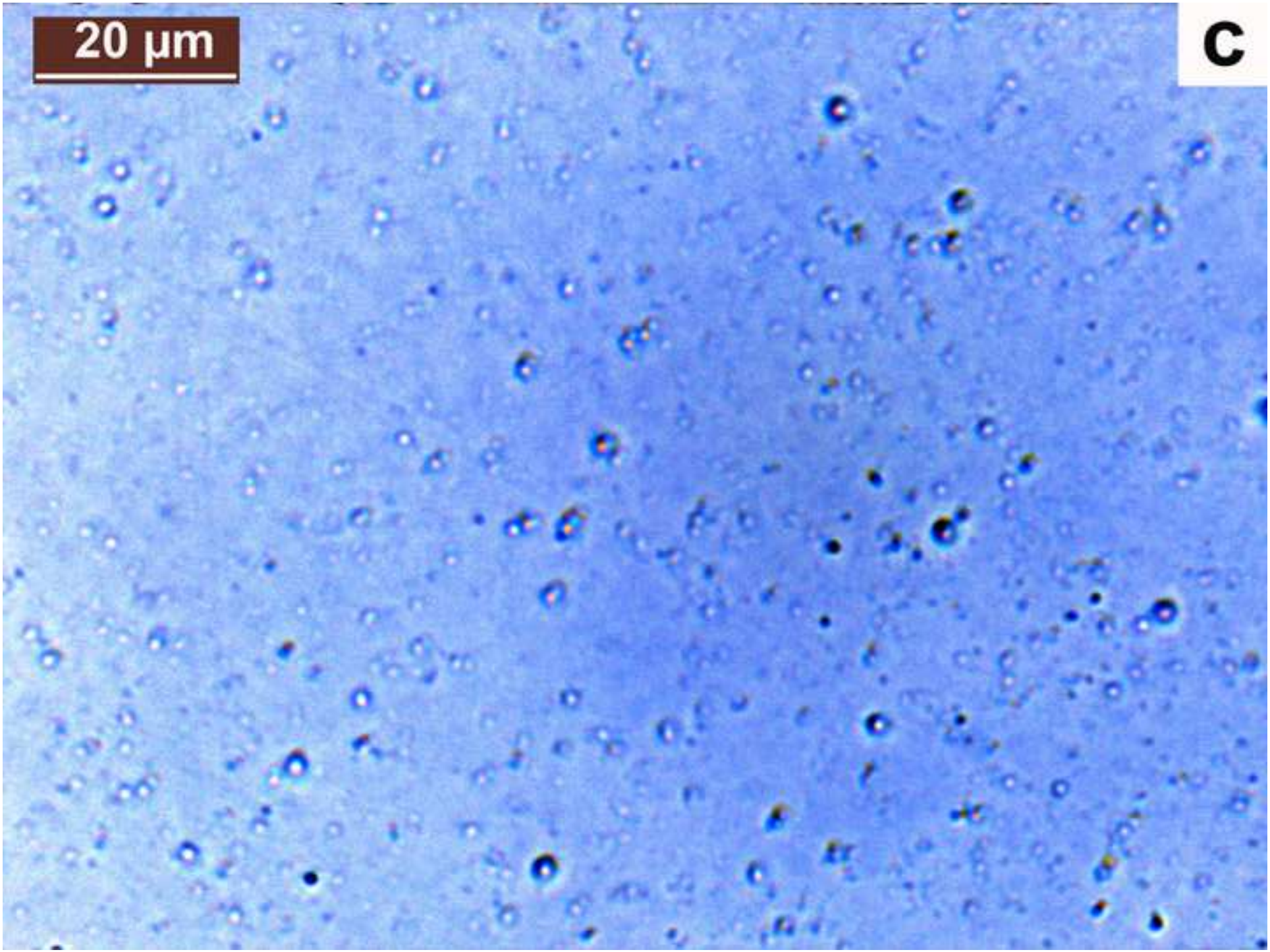

Figure

Click here to download high resolution image

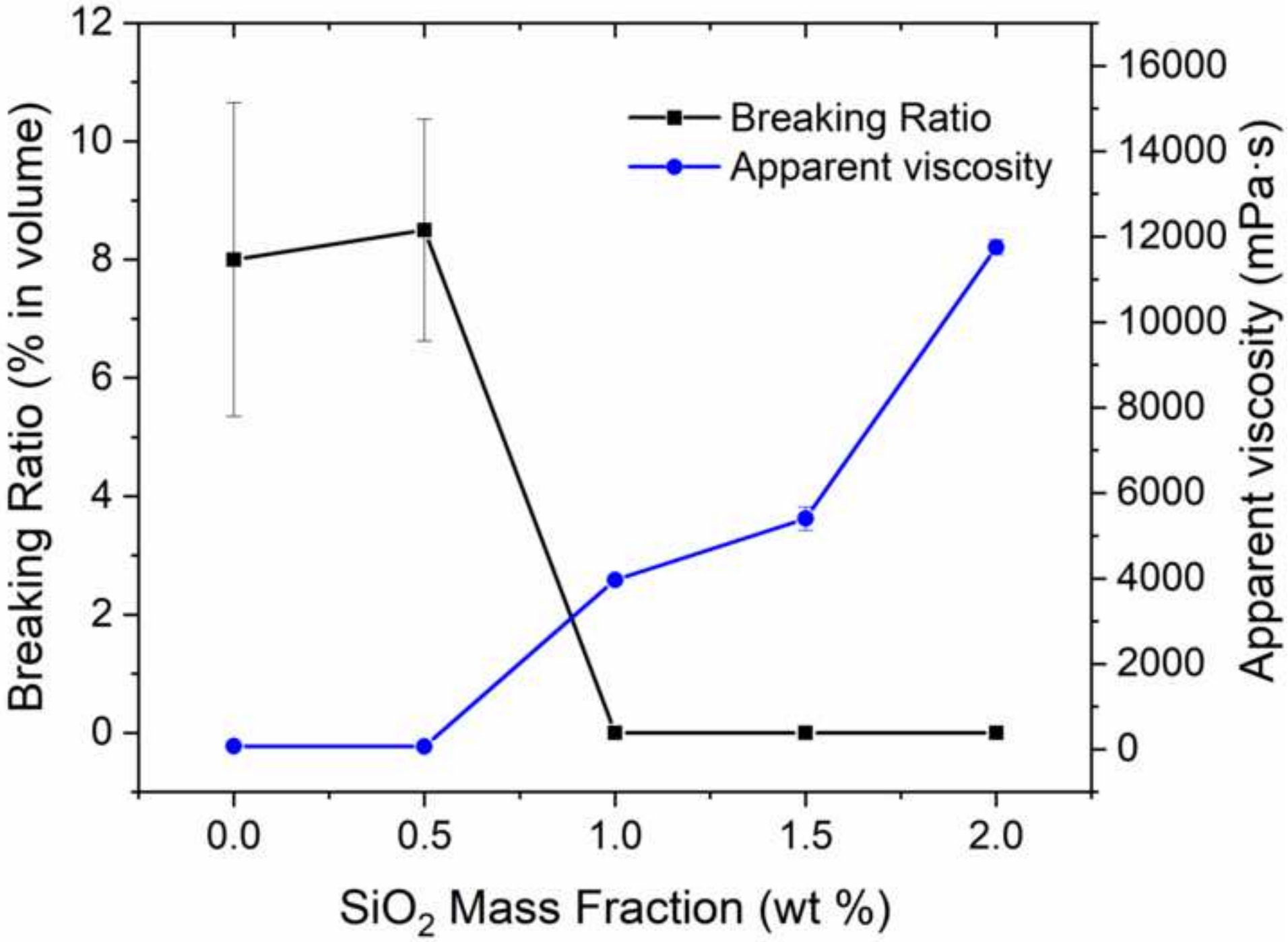

Figure

Click here to download high resolution image

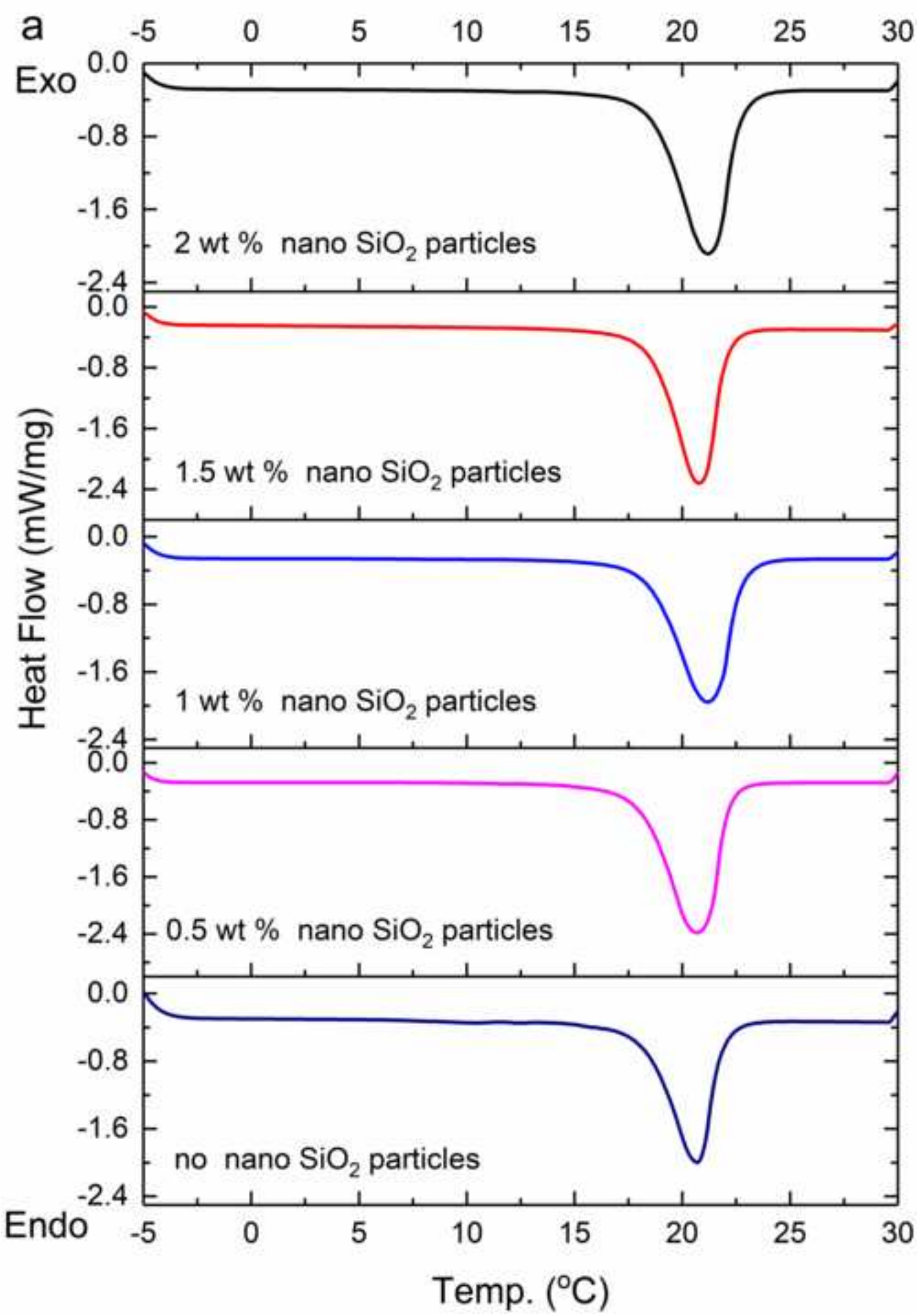

Figure

Click here to download high resolution image